IJC
International Journal of Cancer

Dopamine receptor type 2 (DRD2) and somatostatin receptor type 2 (SSTR2) agonists are effective in inhibiting proliferation of progenitor/stem-like cells isolated from nonfunctioning pituitary tumors

E. Peverelli[1,2], E Giardino[1,2], D. Treppiedi[1,2], M. Meregalli[3], M. Belicchi[3], V. Vaira[4,5], S. Corbetta[6], C. Verdelli[7], E. Verrua[1,2], A. L. Serban[1,2], M. Locatelli[8], G. Carrabba[8], G. Gaudenzi[9], E. Malchiodi[1,2], L. Cassinelli[3], A. G. Lania[10], S. Ferrero[4,11], S. Bosari[4,12], G. Vitale[9,13], Y. Torrente[3], A. Spada[1,2] and G. Mantovani[1,2]

[1] Endocrine Unit, Fondazione IRCCS Ca' Granda Ospedale Maggiore Policlinico, Milan, Italy
[2] Department of Clinical Sciences and Community Health, University of Milan, Milan, Italy
[3] Stem Cell Laboratory, Department of Pathophysiology and Transplantation, University of Milan, Fondazione IRCCS Ca' Granda Ospedale Maggiore Policlinico, Centro Dino Ferrari, Ystem Srl, Milan, Italy
[4] Division of Pathology, Fondazione IRCCS Ca' Granda-Ospedale Maggiore Policlinico, Milan, Italy
[5] Istituto Nazionale Genetica Molecolare "Romeo ed Enrica Invernizzi" (INGM), Milan, Italy
[6] Endocrinology Service, Department of Biomedical Science for Health, University of Milan, IRCCS Istituto Ortopedico Galeazzi, Milan, Italy
[7] Laboratory of Experimental Endocrinology, IRCCS Istituto Ortopedico Galeazzi, Milan, Italy
[8] Neurosurgery Unit, Fondazione IRCCS Ca' Granda Ospedale Maggiore Policlinico, Milan
[9] Department of Clinical Sciences and Community Health, University of Milano, Milan, Italy
[10] Endocrine Unit, IRCCS Istituto Clinico Humanitas, Department of Biomedical Sciences, Humanitas University, Rozzano, Italy
[11] Department of Biomedical, Surgical and Dental Sciences, University of Milan Medical School
[12] Department of Pathophysiology and Transplantation, University of Milan, Milan, Italy
[13] Endocrine and Metabolic Research Laboratory, Istituto Auxologico Italiano-IRCCS, Milan, Italy

Molecular Cancer Biology

The role of progenitor/stem cells in pituitary tumorigenesis, resistance to pharmacological treatments and tumor recurrence is still unclear. This study investigated the presence of progenitor/stem cells in non-functioning pituitary tumors (NFPTs) and tested the efficacy of dopamine receptor type 2 (DRD2) and somatostatin receptor type 2 (SSTR2) agonists to inhibit *in vitro* proliferation. They found that 70% of 46 NFPTs formed spheres co-expressing stem cell markers, transcription factors (DAX1, SF1, ERG1) and gonadotropins. Analysis of tumor behavior showed that spheres formation was associated with tumor invasiveness (OR = 3,96; IC: 1.05–14.88, $p = 0.036$). The *in vitro* reduction of cell proliferation by DRD2 and SSTR2 agonists ($31 \pm 17\%$ and $35 \pm 13\%$ inhibition, respectively, $p < 0.01$ vs. basal) occurring in about a half of NFPTs cells was conserved in the corresponding spheres. Accordingly, these drugs increased cyclin-dependent kinase inhibitor p27 and decreased cyclin D3 expression in spheres. In conclusion, they provided further evidence for the existence of cells with a progenitor/stem cells-like phenotype in the majority of NFPTs, particularly in those with invasive behavior, and demonstrated that the antiproliferative effects of dopaminergic and somatostatinergic drugs were maintained in progenitor/stem-like cells.

Key words: tumor stem cells, pituitary adenomas, dopamine, somatostatin, drug resistance
Additional Supporting Information may be found in the online version of this article.
Grant sponsor: Grant AIRC (Associazione Italiana Ricerca Cancro) to G.M.; **Grant number:** IG 2014–15507; **Grant sponsor:** Italian Ministry of Health
DOI: 10.1002/ijc.30613
History: Received 29 July 2016; Accepted 12 Jan 2017; Online 24 Jan 2017
Correspondence to: Peverelli Erika, PhD, Endocrinology and Diabetology Unit, Fondazione IRCCS Ca' Granda - Pad.Granelli, Via F. Sforza, 35, 20122-Milan, Italy, Tel.: +39 02 55033512, Fax: +39 02 55033361, E-mail: erika.peverelli@guest.unimi.it

Introduction

Recently, a subpopulation of progenitor/stem cells has been demonstrated to exist in pituitary tumors. In particular, these cells were characterized by the expression of stem cells markers, the ability to grow as rounded cell spheres and to self-renew.[1–4] Based on the cancer stem cell hypothesis, tumors develop from a small subpopulation of self-renewing cells, that are able to differentiate into the heterogeneous lineages of the cancer cells and to regenerate the tumor, and are resistant to conventional chemotherapeutic agents. To date the tumor-initiating and tumor-driving role of progenitor/stem cells identified in pituitary tumors has yet to be proven. Neurosurgery by the transphenoidal approach is the treatment of choice for clinically non-functioning pituitary tumors

What's new?
One third of pituitary tumors are non-functioning (NFPTs) producing, but not secreting, gonadotropins, or gonadotropin hormone subunits. Here the authors isolated from the majority of NFPTs, particularly those with invasive behavior, progenitor/stem-like cells co-expressing stem cell markers, embryonic pituitary transcription factors and gonadotropins. These cells reproduced anti-proliferative responses to dopamine and somatostatin analogues observed with bulk tumor cells, underscoring their relevance in the adjuvant medical therapy of NFPTs.

(NFPTs), a tumor type mainly derived from gonadotroph lineage mostly synthesizing but rarely secreting gonadotropins or gonadotropin hormone subunits, that represents one-third of pituitary tumors. Due to incomplete tumor removal and tumor regrowth, adjuvant therapies are required in most cases. Since most NFPTs express both dopamine (DA) receptor type (DRD2)[5–7] and somatostatin (SS) receptors, in particular SS receptor type 2 (SSTR2)[7–9], the use of DA and SS analogs, whose efficacy in other types of pituitary tumors is well established, has been proposed. *In vitro* experiments have demonstrated that specific agonists of DRD2 and SS analogs exert cytostatic and cytotoxic effects in cultured cells from NFPTs.[7,10,11] However, contrasting data are present in literature on tumor shrinkage after treatment with these agents. DRD2 agonists have been demonstrated to be ineffective[12] or effective in a variable percentage of patients[5,6,13–15] in reducing tumor mass. Similarly, SS analogs have been reported to display even more limited effects on tumor growth,[16–18] although a stabilization of tumor remnant from NFPTs after long acting octreotide treatment has been described.[19]

To date, the molecular basis of NFPTs resistance to DRD2 agonists and SS analogs are largely unknown.

The aims of the present study were to test the presence of a population of progenitor/stem cells in NFPTs, to phenotypically characterize them for stem-cell markers expression, biological behavior and *in vivo* tumorigenicity, and to correlate their presence to tumor clinical features. Finally, we seek a role of NFPT progenitor/stem cells in the onset of tumor resistance to dopaminergic and somatostatinergic drugs.

Material and Methods

Patients

The study was approved by the local Ethics Committee and each patient gave informed consent to the use of his/her tumor sample and clinical information. The study was carried on NFPTs removed by transphenoidal surgery from 46 patients with a sellar lesion in the absence of sign or symptom of hormone hypersecretion (28 males and 18 females, age at diagnosis 60.3 ± 16.1 years). On the basis of immunochemistry analysis, 12 were silent gonadotrophs adenomas, 25 null cell adenomas, 4 NFPTs silent corticotrophs adenomas, 3 silent somatotroph and 2 silent somatolactotrophs adenomas.

Magnetic resonance imaging (MRI) showed a macroadenoma (diameter ≥ 10 cm) in all patients, with extrasellar extension in 42, and invasion of the cavernous sinus in 27 cases by radiological and surgical findings. According with the Ki67 index, 9 were atypical adenomas with a Ki67 labeling index ≥ 3 (Supporting Information Table 1 and Table 1).

Pituitary cell culture

Human pituitary tumors were obtained by the transsphenoidal route. Tissues were partially frozen for subsequent molecular analysis and partially enzymatically dissociated in DMEM containing 2 mg/mL collagenase (Sigma-Aldrich, St. Louis, MO, USA) at 37°C for 2 hr, as previously described.[7] Bulk tumor differentiated cells were grown in standard medium (DMEM, 10% fetal bovine serum (FBS), 100 units/mL penicillin, 100 mg/mL streptomycin and 0.25 μg/mL fungizone). To obtain spheres, tumor cells were then resuspended in stem cell permissive medium (serum-free DMEM/F12 1:1 medium) in the presence of 20 ng/mL basic fibroblast growth factor (bFGF), 20 ng/mL epidermal growth factor (EGF), B27, 100 units/mL penicillin, 100 mg/mL streptomycin and 0.25 μg/mL fungizone. DMEM, DMEM/F12 and FBS were from Gibco-Invitrogen (Life Technologies Inc., Carlsbad, CA, USA), bFGF and EGF were from PeproTech EC (London, UK), B27 and fungizone were from Gibco-Invitrogen, pen/strep were from Sigma-Aldrich (St. Louis, MO, USA). bFGF, EGF and B27 were added every week. Cells were plated at a density of 100,000 cells/mL. In a subset of tumors ($n = 3$), sphere-forming efficiency (SFE) was calculated as the percentage of spheres formed after 2 weeks in culture in stem cell permissive medium over the number of plated cells (100 cells/well).

To test the potential for self-renewal, primary spheres were mechanically dispersed in single cells, accurately checked under microscopic examination for single cellularity to exclude that undispersed clumps remained and only the wells containing single cells or irregular aggregates of few cells were considered for the experiment. Cells were then seeded at 10,000 cells/mL and cultured to check the generation of secondary spheres.[20] For clonogenity assays primary spheres were dissociated and cells were plated at a density of 1 cell/well in 96-well plate. Single wells were checked under microscope for the presence of a single cell and marked. After 2 weeks of culture in stem cell permissive medium, marked wells were checked for sphere formation. The

Table 1. Clinical, neuroradiological and anatomopathological features of NFPTs forming or not (pituisphere + or −, respectively) pituispheres in culture

	All patients	Pituisphere + (32 pz)	Pituisphere – (14 pz)	*p* values
Gender (M/F)	28/18	18/14	10/4	0.33
Age at diagnosis (mean ± SD)	60.3 ± 16.1	62.2 ± 16.1	56.0 ± 15.7	0.23
Tumor size (mean ± SD)	24.2 ± 7.2	23.4 ± 6	25.8 ± 9.3	0.39
Extrasellar extension (y/n)	42/4	29	13	0.64
Cavernous sinus invasion (y/n)	27/19	22	5	0.03
Ki 67 (mean ± SD)	1.8 ± 1.56	1.79 ± 1.73	1.82 ± 1.13	0.96
Ki 67 ≥ 3%	9	5	4	0.30
LH/FSH+	12	9	3	0.97

y, yes; n, no.

number of sphere containing wells counted was divided by the number of single cell-containing seeded wells and multiplied by 100.

Spheres size was measured by Axiovision Rel 4.8 software. The diameter of at least 15 different spheres for each tumor was measured.

Flow cytometry

We tested the presence of mesenchymal stem cells (CD90+ CD105+ CD34−),[21] hematopoietic stem cells (CD34+ CD45+), and endothelial cells (CD31 + CD146+) by flow cytometry. Spheres obtained from five tumors (Supporting Information Table 1) and collected after 4 weeks of culture were mechanically dispersed to single-cell suspension. For five-colors flow cytometry, 100,000 cells were resuspended in phosphate-buffered saline (PBS) and incubated with anti-CD133-phycoerythrin (anti-CD133-PE), anti-CD34-APC (Miltenyi Biotec, Bergisch Gladbach, Germany), anti-CD31-FITC, anti-CD105-PE, anti-CD45-APC-CY7, anti-CD90 (thymocyte antigen 1(Thy1))-PE, anti-CD146-PE (BD Biosciences-Pharmingen, San Diego, California, USA). The controls were isotype-matched mouse immunoglobulines. After each incubation performed at 4°C for 20 minutes, cells were washed in PBS containing 1% heat-inactivated FCS and 0,1% sodium azide. The cytometric analysis were done with a Cytomic FC500 flow cytometer and CXP 2.1 software (BC Beckman Coulter). Each analysis included at least 20,000–50,000 events for each gate. A light-scatter gate was set up to eliminate cell debris from the analysis. The percentage of positive cells was assessed after correction for the percentage reactive to an isotype control conjugated. The 7-AAD was added to exclude non-viable cells from the analysis.

RT-PCR analysis

Total RNA was extracted with Trizol Reagent (Life Technologies Inc., USA), using manufacturing protocol, from tissue samples, bulk tumor differentiated cells grown in standard medium or spheres collected after 4 weeks of culture in stem cell permissive medium (Supporting Information Table 1). First strand cDNA was prepared by using Super Script III First Strand Synthesis System (Life Technologies, USA), starting from 2 μg total RNA with oligo(dT)$_{12–18}$ primers. PCR was performed under the following conditions: 94° 5 min, then 35 cycles at 92° 1 min, T_m 1 min, 72° 5 min. *SOX2, EGR1, KLF4, POU5F1/OCT4, SF1, DAX1*, *DRD2, SSTR2, SSTR5,* alpha subunit, *LH* and *FSH* genes were analyzed. We also determined the expression of the human-specific β-actin housekeeping gene for each sample. Specific primer sequences are shown in Supporting Information Table 2.

Immunofluorescence analysis

Spheres obtained from a subset of tumors (Supporting Information Table 1) were collected after 4 weeks of culture and seeded on poly-L-lysine coated glass over/night, then fixed in paraformaldehyde for 4 min and permeabilized for 5 min with 0.1% Triton X-100 in PBS. Cells were then incubated with primary antibodies against PROP1 (1:50; Santa Cruz, (C-15): sc-18468, goat polyclonal), SOX2 (1:20; Millipore, AB5603, rabbit polyclonal) and Nestin (1:50, BD Biosciences, 611658, mouse) 2 hr at room temperature. After washing with PBS, cells were incubated with secondary antibodies 488- and 594-coniugated IgG (Thermo Fisher Scientific, Goat anti-mouse or anti-rabbit) for 1 hr at room temperature and examined by the Leica TCS SP2 confocal system (Leica, Germany).

Immunohistochemistry for progenitor/stem-like cells markers

Immunohistochemistry was performed on sections of paraffin-embedded NFPTs surgically removed from 11 patients and on spheres obtained from a subset of tumors (Supporting Information Table 1) cytospinned on charged slides after 4 weeks of culture. Samples immunoreactivity was analyzed with specific primary antibodies for SOX2 (1:100, Cell Signaling, Danvers, MA, D6D9, rabbit monoclonal), S100 beta (1:10,000, Abcam, Cambridge, UK, EP1576Y, ab52642, rabbit monoclonal), luteinizing hormone (LH, 760-2802, rabbit polyclonal), follicle-stimulating hormone (FSH,

760-2710, rabbit polyclonal), or Ki67/Mib1 proliferation antigen (Ki-67 30-9, rabbit monoclonal) (LH, FSH and Ki67 prediluted from Ventana Medical Systems, Inc., Roche Group, AZ, USA) using an automated immunostainer (BenchMark ULTRA, Ventana Medical Systems Inc) as previously described.[22] Negative controls were prepared in the absence of primary antibody and included in each reaction. For single antigen staining, reactions were revealed using the ultraView Universal DAB (Ventana Medical Systems Inc), whereas for double immunohistochemistry stainings (SOX2/LH or SOX2/FSH) the ultraView Universal Alkaline Phosphatase Red Detection Kit was used after DAB to reveal the second antigen following the manufacturer protocol (Ventana Medical Systems Inc). All slides were counterstained with hematoxylin and scored by light microscopy by two independent observers (VV and SF).

Cell proliferation assay

Cell proliferation was assessed by colorimetric measurement of 5-bromo-2-deoxyuridine (BrdU) incorporation during DNA synthesis in proliferating cells according to the instruction of the manufacturer, as previously reported.[7] Briefly, cells were incubated for 72 h at 37°C with specific DRD2 agonist BIM53097 or SSTR2 agonist BIM23120 (kindly provided by Biomeasure Incorporated/IPSEN, Milford, MA, USA) and then with BrdU at 37°C for 24 h to allow BrdU incorporation in place of thymidine in newly synthesized cellular DNA. At the end of the incubation, culture medium is removed, cells are fixed, DNA is denatured, and the peroxidase-labeled anti-BrdU is added to each well. The immune complexes are detected by the subsequent reaction with the substrate 3,3′,5,5′–tetramethylbenzidine (TMB), and the resultant color read in a microplate spectrophotometer at 450 nm. The absorbance values correlate directly to the amount of DNA synthesis and thus to the number of proliferating cells. A non-specific binding control, in which cells are incubated without BrdU, was added in each experiment. The experiments were performed on cells derived from tumor tissues ($n = 14$) immediately after dispersion prior to sphere formation (Day 3) (50,000 cells/well) and on cells derived from dissociation of spheres collected at Day 30. The spheres were dissociated, cells were counted and seeded at the same density (50,000 cells/well) for the proliferation assay. Moreover, proliferation experiments were performed at different time points (1, 2, 3 and 4 weeks) on both cells grown in complete medium and cells grown in stem cell permissive medium ($n = 3$ tumors).

All experiments were performed once for each primary culture tested and each determination was done at least in triplicate.

In vivo tumor model

Spheres derived from 2 NFPTs (Supporting Information Table 1) and cultured for 2 weeks in stem-cell permissive medium were xenografted in zebrafish embryos, as previously reported.[23,24] We used the *Tg(fli1a:EGFP)*^{y1} transgenic line of zebrafish (*Danio rerio*) expressing EGFP in the entire vasculature. Embryos, collected by natural spawning, were staged and raised at 28°C in fish water (Instant Ocean, 0.1% methylene blue), according to National (Italian D.lgs 26/2014) and European laws (2010/63/EU and 86/609/EEC). Dechorionated embryos at 48 h postfertilization (hpf) were anesthetized with 0.04 mg/mL of tricaine (Sigma-Aldrich). Spheres obtained from NFPTs were mechanically dissociated in single cells and labeled with a red fluorescent dye for cell viability (CellTracker^{TM} CM-DiI, Invitrogen). Cells were then resuspended in PBS and implanted in the sub-peridermal space, close to the sub-intestinal vessels (SIV) plexus, of 48 hpf Tg(fli1:EGFP)y1 zebrafish embryos (100 cells for each embryo). Fishes were observed and imaged 2 h after the injection in order to exclude from the analysis embryos showing cells into the yolk sac and/or in the vasculature. Correctly grafted embryos were incubated at 32°C. A control group, represented by zebrafish injected with PBS only, was included.

At 24 hr post injection (hpi) the presence of circulating grafted cells along the body, the formation of micrometastasis, and the vasoproliferative response triggered by the tumor xenografts were evaluated through a fluorescence stereomicroscope (Leica DM6000B equipped with LAS Leica imaging software). The spread throughout the embryo body was quantified by the "Analyze Particle" plugin of Fiji software, comparing results at 0 and 24 hr post injection (hpi).[25] At least 20 correctly grafted embryos were analyzed in independent experiments.

p27 and CD3 immunoblotting

Spheres were cultured for 4 weeks, and then incubated with or without specific agonists for DRD2 and SSTR2 for 48 h to test the effects on p27 expression or for 3 h to test the expression of CD3. Cells were then lysed in lysis buffer in the presence of protease inhibitors. Proteins were separated on SDS/polyacrylamide gels and transferred to a nitrocellulose filter. 1:100 dilution of anti p27 antibody (Santa Cruz Biotechnology, Santa Cruz, CA, sc-1641, mouse monoclonal) or 1:2000 dilution of anti-cyclin D3 antibody (Cell Signalling, Danvers, MA, #2936, mouse monoclonal) were used. GAPDH was used as housekeeping. Chemiluminescence was detected using the ChemiDoc-IT Imaging System (UVP, Upland, CA) and analyzed using the image analysis program NIH ImageJ.

Statistical analysis

The results are expressed as the mean ± SD. A paired two-tailed Student's *t test* was used to detect the significance between two series of data. Clinical and pathological variables were reported as mean and standard deviation when continuous (age at diagnosis, tumor size), or count when dicothomous (sex, sellar involvement, Ki67 index). Comparisons between groups forming and non-forming spheres were made by Student's *t test* or Fisher's for continuous and

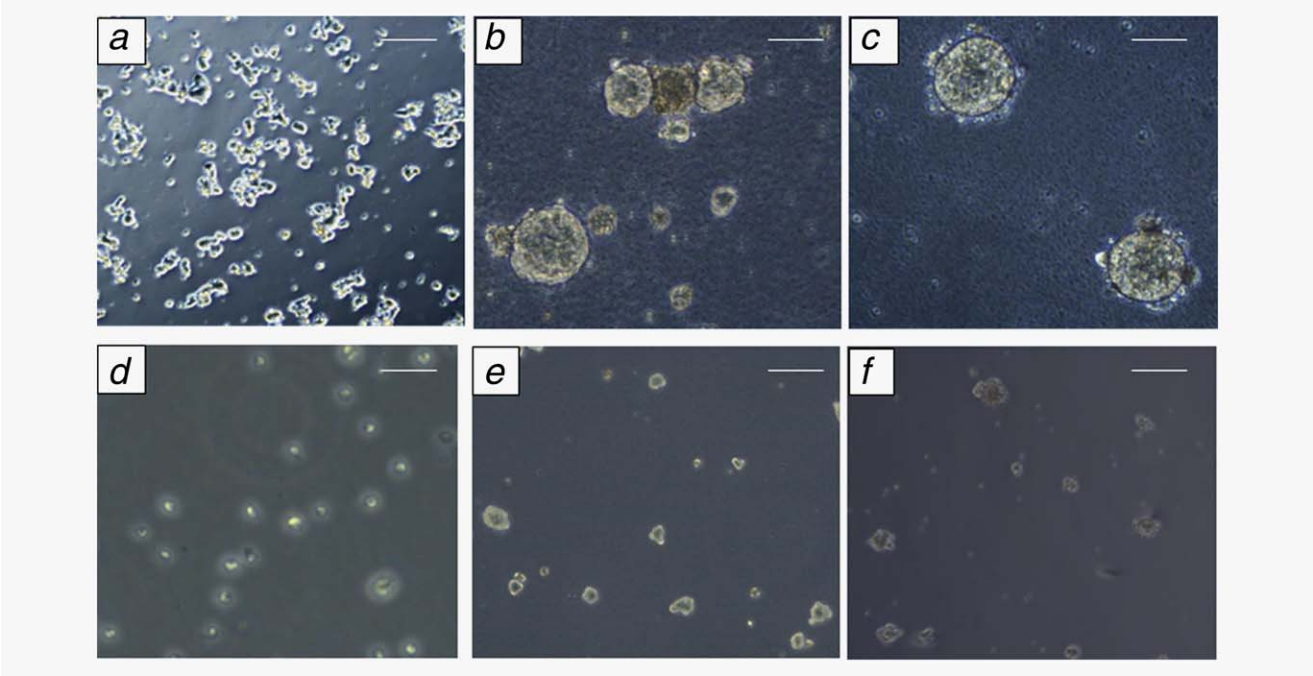

Figure 1. Representative pictures of spheres isolated from cultured NFPTs. (***A***) Aggregates of tumor cells 1 day after tumor dispersion and cell seeding. (***B***) The spheres appeared after 2 weeks of culture in stem cell-permissive medium. (***C***) Spheres dimensions remained nearly unchanged after 5 weeks of culture. (***D***) Primary spheres dissociated into single cells and seeded in stem cells permissive medium. (***E***) Secondary spheres appeared the day after seeding of cells with morphology similar to primary spheres, but lower size. (***F***) Secondary spheres did not significantly grow after 2 weeks in culture. Scale bar 50 μm. [Color figure can be viewed at wileyonlinelibrary.com]

categorical variables, respectively. $p < 0.05$ was accepted as statistically significant. Statistical analysis was performed by SPSS version 21.0 statistical package (SPSS Inc, Chicago, IL).

Results

Isolation and characterization of spheres from cultured NFPTs

Tumor cells derived from NFPTs normally grow in suspension as irregular aggregates, without formation of spheres in standard culture conditions (DMEM + 10% FBS medium) (Fig. 1 panel *A*). About 2 weeks after cell seeding in stem cell permissive medium nonadherent round cell spheres appeared in 69.6% of cultured NFPTs ($n = 46$) (Fig. 1, panel *B*, *C*). Sphere-forming efficiency (SFE) calculated in a subset of tumors ranged from 2% to 5%. Secondary spheres were obtained from disaggregated primary spheres seeded at low density, suggesting that they are able to self-renew (Fig. 1, panel *D*–*F*). Moreover, clonogenicity assay in which cells from dissociated primary spheres were plated at a density of 1cell/well in 96-well plate revealed an efficiency of spheres formation ranging from 3.8 to 7.7%. No spheres were obtained from the dissociated secondary spheres.

To quantify the specific cell populations, we tested the primary spheres by FACS for the expression of groups of markers. A variable proportion of cell populations expressed the stem cells associated markers CD90 ($22.8 \pm 30.9\%$), whereas $CD90^{+}$ $CD105^{+}$ $CD34^{-}$ mesenchymal stem cells represented $3.3 \pm 1\%$ of the sphere population. Spheres were prevalently CD45 negative ($0.84 \pm 0.51\%$ of positive cells), ruling out a consistent contribution of cells deriving from blood. A poor, if any, contribution of vascular-endothelial progenitors is suggested by the very low percentage of cells expressing CD31 ($1.88 \pm 3.54\%$), CD146 ($1.26 \pm 1.02\%$) or CD133 ($0.76 \pm 0.48\%$), the hematopoietic/endothelial stem marker and a marker for cancer stem cells in different tumors.

Qualitative RT-PCR analysis showed that spheres expressed *SOX2, POU5F1/OCT4* and *KLF4* pluripotent cell-specific transcription factors together with transcription factors involved in gonadotroph differentiation, such as *DAX1, SF1* and *EGR1*, and gonadotropin subunits (alpha subunit, *LH* and *FSH*; Fig. 2*A*). In contrast to the strong expression observed in spheres, the expression of *POU5F1/OCT4* in differentiated cells (*i.e.*, cells cultured in complete standard medium) of the corresponding tumors was nearly undetectable or very low (Fig. 2*B*).

Immunohistochemistry analysis of spheres (Fig. 2*C*) confirmed that a small proportion of cells were positive for SOX2, mainly with nuclear localization. LH positive cells ranged from 10% to 35% of sphere cells, with a cytoplasmic staining, while the marker of folliculostellate cells S100beta[26] was undetectable. A variable proportion of cells within the spheres obtained from different tumors displayed nuclear Ki67 staining (from 1% to 10%).

Immunofluorescence analysis (Fig. 2*D*) confirmed the positivity of spheres for SOX2, with some variability in the percentage of SOX2 positive cells and in the nuclear or

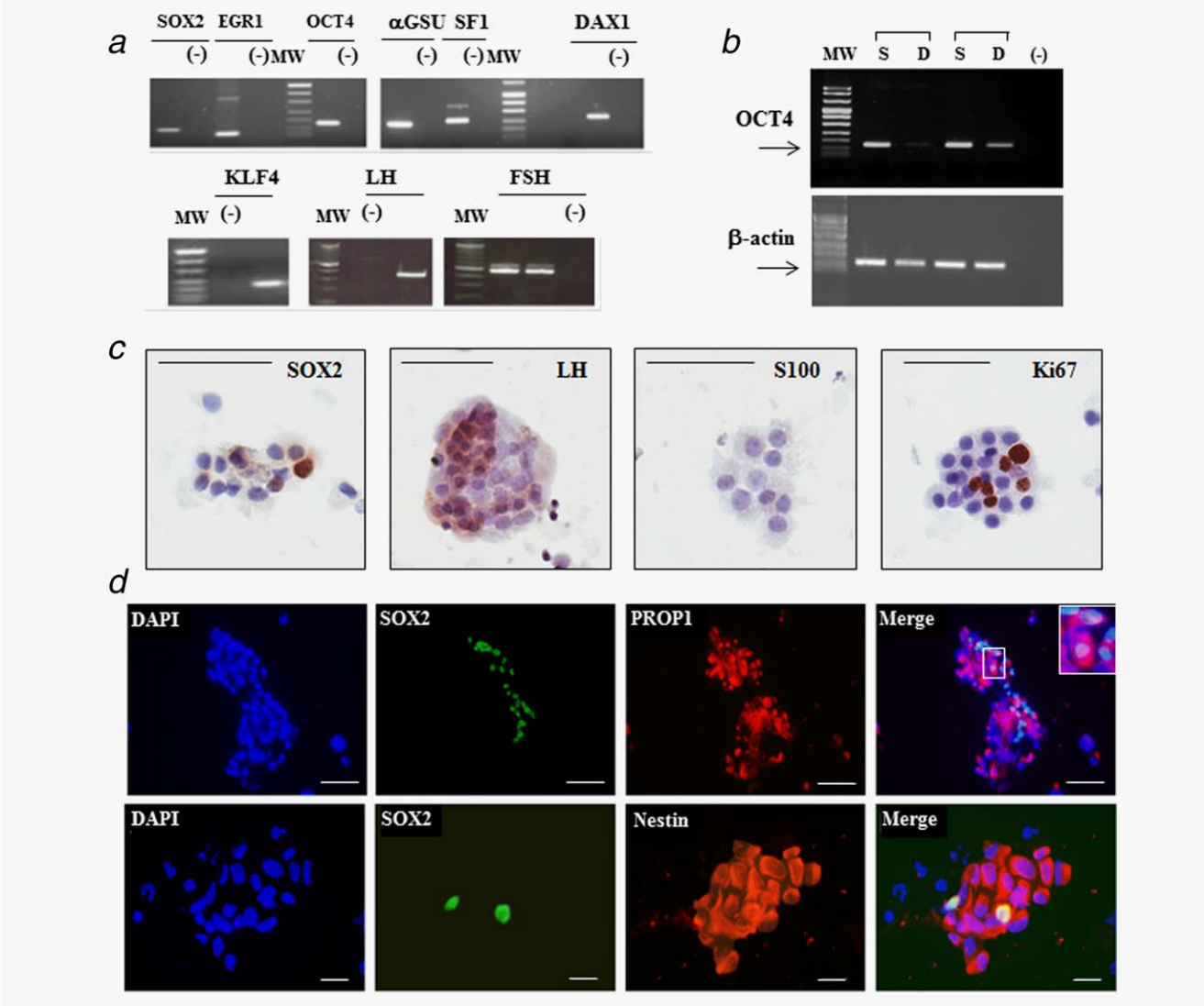

Figure 2. Spheres express mRNA of progenitor/stem cells and embryonic pituitary-related factors. (***A***) Representative RT-PCR analysis performed on spheres derived from a cultured NFPT. MW, molecular weight marker; (−), negative control. (***B***) Representative RT-PCR analysis performed on both spheres (S) and bulk tumor differentiated cells grown in standard medium (D) derived from two different NFPTs. MW, molecular weight marker; (−), negative control. (***C***) Representative pictures of immunohistochemistry analysis performed on spheres derived from a cultured NFPT. Staining for SOX2, LH, S100 and Ki67are shown (20× magnification). Scale bar 50 μm. Similar data were obtained in the other analyzed samples. (***D***) Representative immunofluorescence analysis of spheres. Cells were stained for PROP1 (*red*) and SOX2 (*green*) (scale bar 50 μm) or Nestin (*red*) and SOX2 (*green*) (scale bar 15 μm). DAPI (*blue*) was used for nuclei staining. Insert in the "merge" upper panel shows higher magnification.

cytoplasmatic localization between different spheres. Moreover, this analysis revealed the expression of the pituitary specific transcription factor PROP1 (prophet of PIT1) that colocalized with SOX2 in the nucleus of a percentage of cells ranging from 2% to 10%, while it was cytoplasmatic in SOX2 negative cells, suggesting the existence of a heterogeneous population of stem cells (SOX2+/PROP1+) and precursor cells in a transient stage of the differentiation, expressing PROP1 but not SOX2.[27] Finally, our data showed co-expression of nestin in SOX2 positive cells.

Long-term proliferation ability of sphere-forming cells was demonstrated by proliferation assays, showing a detectable BrdU incorporation in newly synthesized DNA in proliferating cells for up to 4 weeks in culture, and by positive Ki67 staining in spheres cultured up to 4 weeks (Fig. 2*C*). In contrast, differentiated cells from the same tumors, grown in complete medium, were actively proliferating only for 1 week (Supporting Information Fig. 1), consistent with the observation that pituitary cells primary cultures usually survive *in vitro* only few days.[4,28]

The *in vivo* tumorigenicity of spheres was assessed in zebrafish model, that allows to test invasive and angiogenic potential of injected cells.[4,23] Sphere-forming cells were disaggregated and xenografted in zebrafish embryos taking advantage of the *Tg(fli1:EGFP)*^{y1} zebrafish line that expresses EGFP

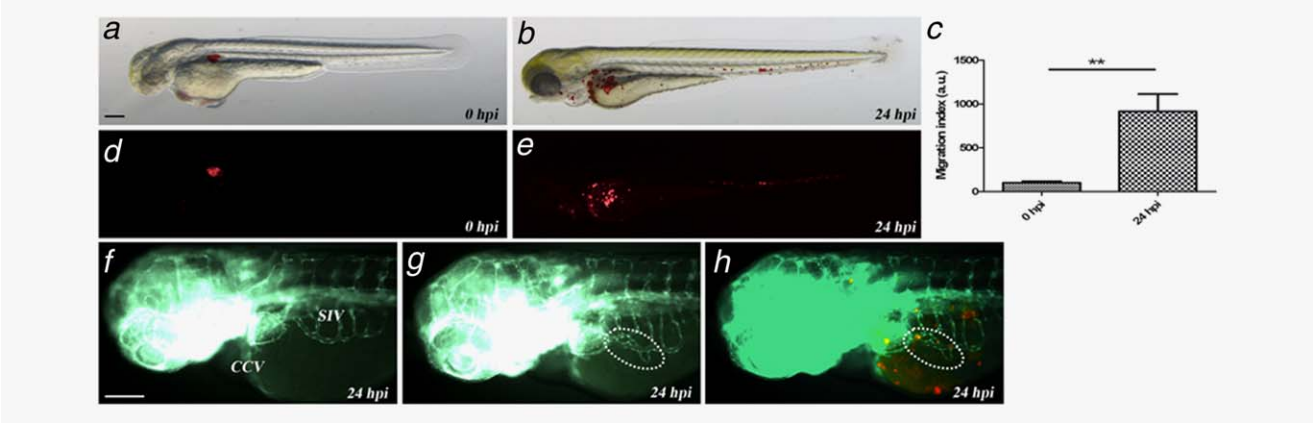

Figure 3. Tumorigenicity of spheres in zebrafish model. (***A–E***) Invasive potential of pituitary tumor derived spheres. Representative pictures of zebrafish embryos at 0 hpi (A–D) and 24 hpi (B–E). A,B: overlay of bright field and fluorescence, D,E: red fluorescent channel. C: Quantification of hPASC invasiveness. The migration index was calculated as the mean number of red clusters in grafted embryos at 0 (a) and 24 hpi (b). (**= $p < 0.01$, *t* test). A strong migration throughout the embryo body of sphere derived cells (red) was observed in all the grafted embryos. (***F–H***) Pro-angiogenic activity of sphere cells. (F) PBS-injected control embryo, (G,H) grafted embryos at 24 hpi. New endothelial structures (white dashed area), sprouting from the SIV, reached the tumor mass (dotted lines). CCV: common cardinal vein. (H) merge of green (EGFP expressed in the vasculature) and red (injected sphere cells) channels. All images were oriented so that rostral is to the left and dorsal is at the top. Scale bars: 100 μm.

in the vascular endothelium. At 24 hpi, tumor cells of both patients migrated out from the site of the injection in every grafted embryos, demonstrating a strong invasive behavior of injected cells (Fig. 3*A–E*). Moreover, injected cells of each patient stimulated the formation of endothelial sprouts from the subintestinal vessels (SIV) plexus in the 30% (patient # 31) and 33% (patient # 32) of grafted embryos, demonstrating their *in vivo* angiogenic potential. In contrast, control embryos did not show alterations in vascular network (Fig. 1*F*). Given that the tumor cells of both patients displayed a similar migration index and pro-angiogenic effect, we reported the results of a representative experiment in Figure 3.

Stem cell markers expression in NFPT tissues

Since a subset of NFPTs was not able to form spheres in culture, we investigated a possible different expression of stem cells markers in tissues of origin.

All tumor tissues analyzed by RT-PCR expressed *SOX2, POU5F1/OCT4* and *KLF4* together with the gonadotrope differentiation marker *EGR1* (Fig. 4*A*). By immunohistochemistry, we found that SOX2 was expressed in about 4% of pituitary cells of NFPT tissues (range 0–9%, Fig. 3*B*) without any difference between tumors that formed or not spheres in culture. SOX2 positive cells were sparsely distributed in the tissue sections, without any apparent preferential localization in proximity of small vessels. Double immunostaining analysis performed in silent gonadotroph tumors showed that the majority of SOX2 positive cells were negative for either LH or FSH, and only 1% of SOX2+ cells presented co-expression of LH (Fig. 4C,*D*).

Correlation of spheres formation with clinical tumor behavior

No difference in clinicopathological or radiological features was found between NFPTs that generated or not spheres *in vitro*. Interestingly Pearson's chi-squared test showed that formation of spheres was positively associated with cavernous sinus invasion (OR = 3,96; IC: 1.05–14.88, $p = 0.036$) (Table 1), whereas no correlation with sex, age, tumor size, Ki67 and extrasellar extension was observed.

DRD2- and SSTR2-mediated antiproliferative effects are maintained in spheres

We first evaluated the expression of *DRD2, SSTR2* and *SSTR5* in spheres and in tumor tissues from which they were derived by RT-PCR. We found that *DRD2* and *SSTR2* mRNAs were expressed in the tissues and in the corresponding spheres, whereas *SSTR5* expression was undetectable in spheres although it was expressed in all tissues analyzed (Fig. 5*A* and data not shown).

We then tested the antiproliferative effects of the specific DRD2 agonist BIM53097 and SSTR2 agonist BIM23120 on cultured cells derived from tumor tissues immediately after dispersion prior to sphere formation (Day 3) and on spheres (Day 30). BrdU incorporation assay showed that in the subset of NFPTs in which DRD2 agonist BIM53097 inhibited cell proliferation (43% of NFPTs tested), the inhibition found in bulk tumor cells ($31 \pm 17\%$ inhibition at 10 nM; $p < 0.01$ vs. basal) was maintained in the corresponding spheres ($45 \pm 24\%$ inhibition, $p < 0.01$ vs. basal). Similarly, BIM23120 reduced cell proliferation both in freshly dispersed tumoral cells (33% of tested NFPTs) and corresponding spheres ($35 \pm 13\%$ and $65 \pm 21\%$ inhibition at 10 nM, $p < 0.01$ and $p < 0.05$ vs. basal, respectively) (Fig. 5*B*). The proliferation rate of spheres derived from resistant NFPTs was not affected by the treatment with the corresponding agonist.

The efficacy of DRD2 and SSTR2 agonists in reducing spheres proliferation was also demonstrated by an increase of

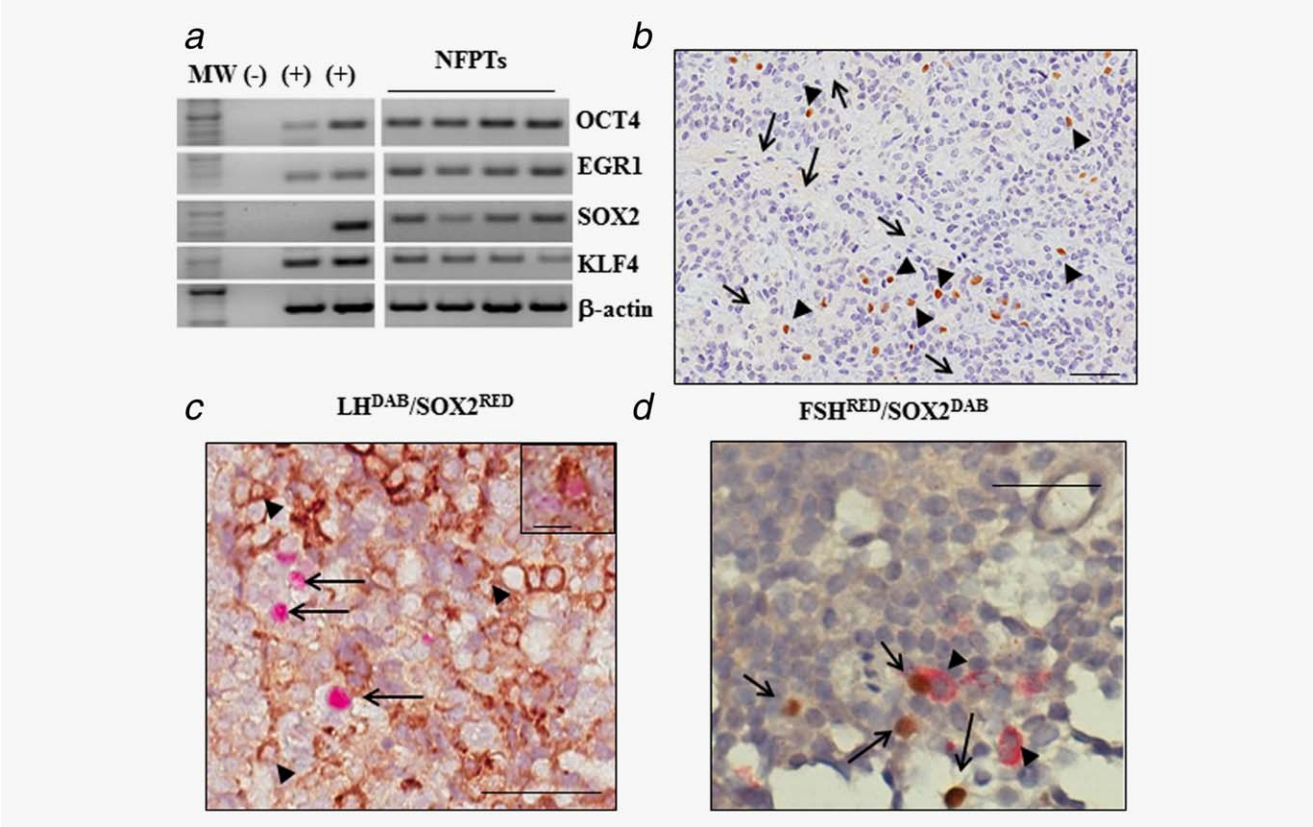

Figure 4. Analysis of stem cell markers expression in NFPT tissues. (***A***) Representative pictures of RT-PCR analysis performed on NFPT tissues. MW, molecular weight marker; (−), negative control; (+), positive controls, human bone-marrow mesenchymal stem cells and MCF7 human breast cancer cell line, respectively. (***B***) Immunohistochemistry analysis in NFPT tissue sections showed sparsely distributed SOX2 positive cells, indicated by arrowheads, without a clear localization in proximity of small vessels (indicated by arrows). A representative picture is shown (20× magnification, scale bar 50 μm). Similar results were found in NFPTs that formed spheres in culture ($n = 6$) or not ($n = 5$). (***C,D***) Double immunohistochemistry staining was performed for SOX2 and LH (C) or FSH (D) proteins in pituitary tumors to investigate co-expression of the stem-cell marker with hormones. Representative images are shown for LH (brown, revealed with DAB, indicated by arrowheads) and SOX2 (red, revealed with alkaline phosphatase, indicated by arrows) or for FSH (red, indicated by arrowheads) and SOX2 (brown, indicated by arrows) (20× magnification, scale bar 50 μm) stainings in a NFPT case. SOX2 positive cells are mostly negative for LH and FSH. The insert in (C) shows a representative picture of a cell positive for both LH and SOX2.

cyclin-dependent kinase inhibitor p27 expression (3.4 ± 0.6 fold over basal, $p < 0.05$) and a decrease in cyclin D3 (CD3) expression ($50 \pm 7\%$ vs. basal, $p < 0.001$) induced in spheres by BIM53097 or BIM23120 after 48 and 3 hr incubation, respectively (Fig. 5*C*).

No difference in the frequency of spheres formation between NFPTs that were *in vitro* resistant or sensitive to DRD2 and SSTR2 agonists was observed. However, the spheres derived from tumors resistant to DRD2 and SSTR2 agonists were larger than those obtained from sensitive NFPTs (mean diameter 70 ± 9 μM and 39 ± 8 μM, respectively, $p < 0.01$) (Fig. 5*D*).

Discussion

The present study confirms the presence of sphere-forming cells co-expressing stem cell and differentiative markers in pituitary tumors and provides new insights into their correlation with tumor behavior and responsiveness to dopaminergic and somatostatinergic agents.

To date, few published studies reported isolation of progenitor/stem cells from dispersed human pituitary tumors by growing tumoral cells in stem-cell permissive medium to obtain non-adherent spheres. These putative parenchymal tumor stem cells expressed stem cell markers, were able to self-renew and had a high efflux capacity.[1–4]

Consistent with the previous observation that stem cell-associated markers are particularly overexpressed by NFPTs,[2,29,30] we observed spheres formation in about 70% of cultured NFPTs, a success rate nearly identical to that obtained by Murth *et al.* in NFPTs and GH-secreting pituitary tumors.[4] The spheres were able to self-renew in culture, although with a limited potential, restricted to secondary spheres, in agreement with published data on spheres derived from both rodent normal pituitary and human pituitary adenomas.[2,31]

FACS-based phenotypic characterization of cells derived from spheres detected a variable proportion of cells expressing different stem markers. In particular, a significant

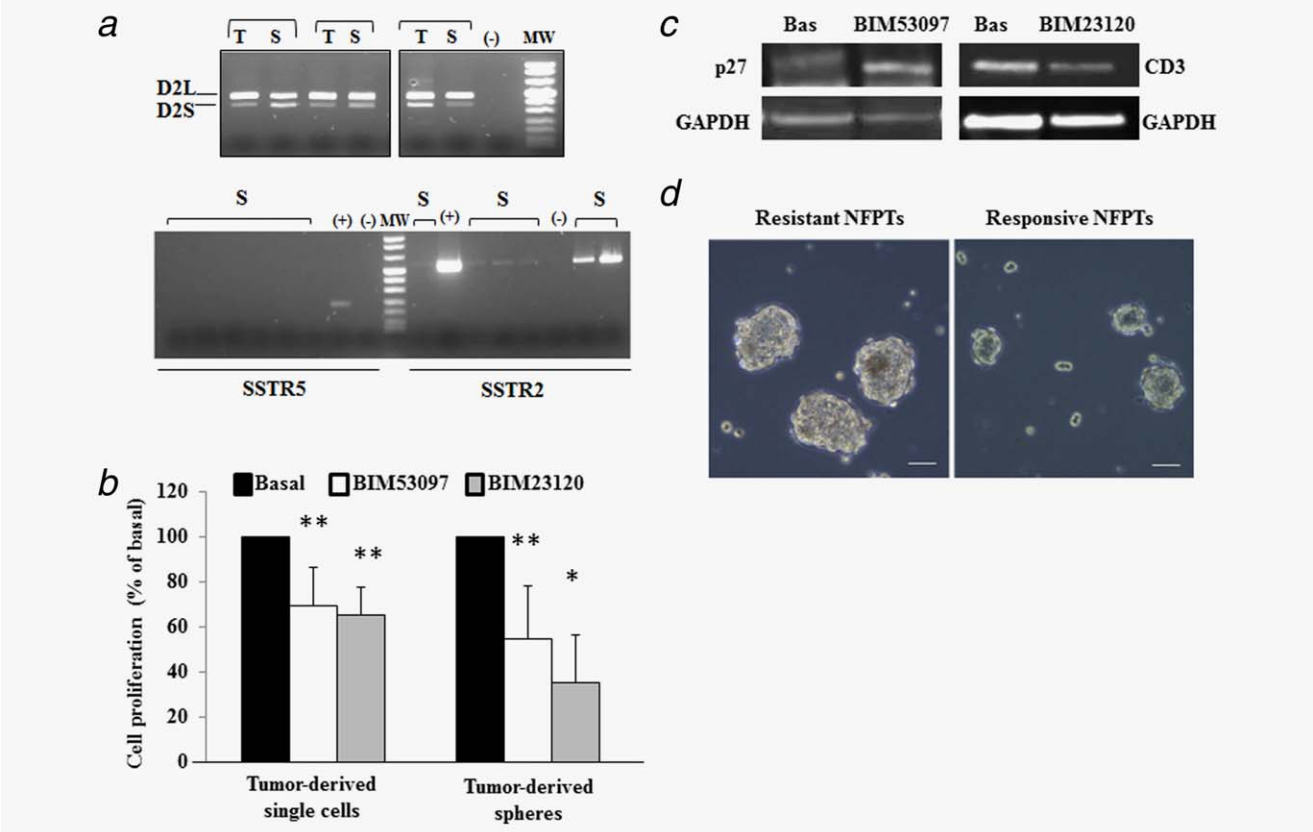

Figure 5. DRD2 and SSTR2 expression and antiproliferative effects are maintained in spheres. (***A***) Representative RT-PCR analysis showing the expression of both splicing variant of *DRD2* (D2L, the long isoform, and D2S, the short isoform) in NFPT tissues (T) and respective spheres (S) (upper panel). Lowe panel: SSTR5 and SSTR2 expression in spheres (S) from different NFPTs is shown. (−), negative control; (+), positive control; MW, molecular weight marker. (***B***) Effect of BIM53097 and BIM23120 treatment (10 nM for 72 h) on proliferation of cells dispersed from NFPTs (Day 3) or spheres (Day 30). The figure includes the data of the subset of NFPTs responsive to treatment with BIM53097 and BIM23120. The inhibition of proliferation was maintained in spheres, with no significant differences between the inhibitory effect on tissue cells and spheres and between the respective basal proliferation rates. Each determination was done at least in triplicate. Values represent mean ± SD, *=$p < 0.05$, **=$p < 0.01$ vs. corresponding basal, *t* test. (***C***) Representative immunoblotting of p27 and CD3 in spheres derived from two different NFPTs. The membranes were stripped and reprobed with GAPDH antibody. Spheres were incubated with or without the indicated agonist for 48 and 3 hr, respectively. (***D***) Representative pictures of spheres derived from a NFPT resistant to both DA and SS analogs and a responsive tumor after 4 weeks of culture (5× magnification, scale bar 50 μm). Resistant tumors-derived spheres were larger than those obtained from responsive NFPTs (mean diameter 70 ± 9 μM and 39 ± 8 μM, respectively, $p < 0.01$). About 6 resistant and 4 responsive tumors were measured (at least 15 different spheres/NFPT). [Color figure can be viewed at wileyonlinelibrary.com]

proportion of cell population expressed the stem cell associated marker CD90, while only a small fraction of cells displayed a mesenchymal stromal stem cell immunophenotype (CD90+ CD105+ CD34−),[21] in contrast with recently published data demonstrating the isolation from pituitary adenomas of a mesenchymal stem cells population.[32] Moreover, the contribution of cells positive for hematopoietic/endothelial antigens, such as CD34, CD45, CD31 and CD146 was very low.

We found a low proportion of cells positive for CD133, considered a common marker of cancer stem cells in different tumors. Previous studies reported the presence of CD133 in pituitary adenomas,[2,30] although in spheres derived from these tumors contrasting data have been reported, showing both CD133 expression[1,4] and low or absent CD133 expression,[2,33] accordingly with the results of the present study.

By the combination of different techniques, sphere forming cells resulted to express several markers of stemness belonging to different categories. In particular, they expressed: (*i*) pluripotent embryonic stem cell markers, such as SOX2, POU5F1/OCT4, KLF4 that together constitute the pluripotency transcription-factor core of embryonic stem cells,[34] and Nestin; (*ii*) embryonic pituitary specific transcription factors involved in gonadotroph differentiation, consistent with gonadotroph origin of most NFPTs, such as DAX1, SF1 and EGR1, a transcription factor required for the activation of LH beta subunit promoter; (*iii*) mature hormones, that is, gonadotropins, and specific receptors, that is, DRD2 and SSTR2. A similar molecular phenotype composed both of a stemness and an embryonic part has been described in stem cells of normal adult pituitary.[35] Conversely, the expression of hormones and receptors by spheres suggests a stage

of committed precursor to a specific cell type, that is, gonadotroph.

Sphere-forming cells displayed unique features in comparison with the bulk of tumor cells, including increased expression of stem cell markers and long-term proliferation ability.

Moreover, they showed tumorigenic potential in zebrafish model, as demonstrated by their invasive behavior and their proangiogenic activity.

The expression of SOX2, POU5F1/OCT4, KLF4 and EGR1 was also found in NFPT tissues. In particular, the presence of SOX2 positive cells in analyzed tissues was independent from the ability to form or not spheres in culture, strongly suggesting the need of other genetic or epigenetic factors to ensure spheres generation.

Statistical analysis showed that formation of spheres was positively associated with cavernous sinus invasion, whereas no statistically significant correlation was found when considering tumor size, extrasellar extension and/or Ki67 proliferative index. Although considered benign, as many as 25–55% of pituitary tumors are invasive and some exhibit clinically aggressive behavior, although a clear definition of aggressiveness and or invasiveness does not exist to date.[36] The latest WHO classification criteria define pituitary tumors by their histological characteristics; however, there is no reliable histological marker or classification system for characterizing aggressive neoplasms yet. Although in the literature "aggressive" is often used synonymously with "invasive," invasiveness should mainly be defined by radiological and surgical findings, such as invasion of surrounding structures, primarily the sphenoid sinus and/or the cavernous sinus. Conversely, aggressive pituitary tumors are characterized by their clinical behavior (expansively growing tumors/high rate of recurrence/resistance to standard treatments, independently of size and invasiveness), together with histopathological findings, such as higher mitotic activity, defined by a Ki67 labeling index $\geq$3% or p53 immunopositivity.[36]

In this scenario, the data presented here suggest that spheres formation is correlated with tumor invasiveness rather than aggressiveness. Since invasion of the cavernous sinus strongly reduces the success of transsphenoidal neurosurgery and is the most common cause of tumor regrowth, these data suggest that tumor stem cells may contribute to tumor recurrence, according to cancer stem cells model.

To investigate if the sphere-forming cells were characterized by a reduced sensitivity to the antiproliferative action of DA and SS, supporting a possible role of this cell population in the NFPTs resistance to DRD2 and SSTR2 agonists, we measured cell proliferation in primary tumor cells and in the corresponding spheres. Our data demonstrated that DRD2 and SSTR2 are expressed by spheres and are functionally coupled to inhibitory pathways, since they mediated reduction of cell proliferation. Moreover, in the subset (about 50%) of tumors that were responsive to DA and SS analogs, the antimitogenic action induced by these agents in bulk tumor cells was maintained unaltered in progenitor/stem-like cells. These data are in agreement with the recently described reduction of cell viability exerted by the somatostatin/dopamine chimera BIM-23A760 in progenitor/stem cells isolated from pituitary tumors.[4]

Consistent with the present results, a recent study reported that dopamine agonist therapy in patients with NFPTs was associated with decreased prevalence of residual tumor regrowth after transsphenoidal surgical resection.[15]

Although the frequency of spheres formation from resistant or sensitive NFPTs was similar, resistant tumors formed larger spheres compared with sensitive ones, reflecting an increased proliferative activity of progenitor/stem cells in these tumors. It is worth noting that several clinical observation indicate that resistance to dopamine agonists observed in very few patients with PRL secreting adenomas is associated with invasive adenomas or even carcinomas.[37] Admittedly, no data on stem/progenitor cells expression in pituitary cancers are available yet.

In conclusion, we provided further evidence for the existence of progenitor/stem-like cells that grow as spheres in culture and express stem cell specific markers and pituitary embryonic transcription factors involved in gonadotrope differentiation in the majority of NFPTs, particularly in those with invasive behavior. Moreover, we demonstrated that in about a half of NFPTs dopaminergic and somatostatinergic drugs are able to reduce proliferation rate of both bulk tumor cells and progenitor/stem cells, thus underlining the need for further clinical trials with these agents in the adjuvant medical therapy of NFPTs.

References

1. Xu Q, Yuan X, Tunici P, et al. Isolation of tumour stem-like cells from benign tumours. *Br J Cancer* 2009;101:303–31.
2. Chen L, Ye H, Wang X, et al. Evidence of brain tumor stem progenitor-like cells with low proliferative capacity in human benign pituitary adenoma. *Cancer Lett* 2014;349:61–6.
3. Mertens F, Gremeaux L, Chen J, et al. Pituitary tumors contain a side population with tumor stem cell-associated characteristics. *Endocr Relat Cancer* 2015;22:481–504.
4. Würth R, Barbieri F, Pattarozzi A, et al. Phenotypical and pharmacological characterization of stem-like cells in human pituitary adenomas. *Mol Neurobiol* 2016 Aug 11. [Epub ahead of print] DOI: 10.1007/s12035-016-0025-x.
5. Vieira Neto L, Wildemberg LE, Moraes AB, et al. Dopamine receptor subtype 2 expression profile in non-functioning pituitary adenomas and in vivo response to cabergoline therapy. *Clin Endocrinol (Oxf)* 2015;82:739–46.
6. Pivonello R, Matrone C, Filippella M, et al. Dopamine receptor expression and function in clinically nonfunctioning pituitary tumors: comparison with the effectiveness of cabergoline treatment. *J Clin Endocrinol Metab* 2004;89:1674–83.
7. Peverelli E, Olgiati L, Locatelli M, et al. The dopamine-somatostatin chimeric compound BIM-23A760 exerts antiproliferative and cytotoxic effects in human non-functioning pituitary tumors by activating ERK1/2 and p38 pathways. *Cancer Lett* 2010;288:170–6.
8. Faglia G, Bazzoni N, Spada A, et al. In vivo detection of somatostatin receptors in patients with functionless pituitary adenomas by means of a radio-iodinated analog of somatostatin. *J Clin Endocrinol Metab* 1991;73:850–6.
9. Taboada GF, Luque RM, Bastos W, et al. Quantitative analysis of somatostatin receptor subtype (SSTR1-5) gene expression levels in somatotropinomas and non-functioning pituitary adenomas. *Eur J Endocrinol* 2007;156:65–74.
10. Florio T, Barbieri F, Spaziante R, et al. Efficacy of a dopamine-somatostatin chimeric molecule, BIM-23A760, in the control of cell growth from

primary cultures of human non-functioning pituitary adenomas: a multi-center study. *Endocr Relat Cancer* 2008;15:583–96.
11. Gruszka A, Kunert-Radek J, Radek A, et al. The effect of selective sst1, sst2, sst5 somatostatin receptors agonists, a somatostatin/dopamine (SST/DA) chimera and bromocriptine on the "clinically non-functioning" pituitary adenomas in vitro. *Life Sci* 2006;78:689–93.
12. Bevan JS, Burke CW. Non-functioning pituitary adenomas donot regress during bromocriptine therapy but possess membrane bound dopamine receptors which bind bromocriptine. *Clin Endocrinol (Oxf)* 1986;25:561–72.
13. Colao A, Ferone D, Lastoria S, et al. Hormone levels and tumour size response to quinagolide and cabergoline in patients with prolactin-secreting and clinically non-functioning pituitary adenomas: predictive value of pituitary scintigraphy with 123I-methoxybenzamide. *Clin Endocrinol (Oxf)* 2000;52:437–45.
14. Lohmann T, Trantakis C, Biesold M, et al. Minor tumour shrinkage in nonfunctioning pituitary adenomas by long-term treatment with the dopamine agonist cabergoline. *Pituitary* 2001;4:173–8.
15. Greenman Y, Cooper O, Yaish I, et al. Treatment of clinically nonfunctioning pituitary adenomas with dopamine agonists. *Eur J Endocrinol* 2016; 175:63–72.
16. de Bruin TW, Kwekkeboom DJ, Van't Verlaat JW, et al. Clinically nonfunctioning pituitary adenoma and octreotide response to long term high dose treatment, and studies in vitro. *J Clin Endocrinol Metab* 1992;75:1310–7.
17. Katznelson L, Oppenheim DS, Coughlin JF, et al. Chronic somatostatin analog administration in patients with alpha-subunit-secreting pituitary tumors. *J Clin Endocrinol Metab* 1992;75: 1318–25.
18. Plockinger U, Reichel M, Fett U, et al. Preoperative octreotide treatment of growth hormone-secreting and clinically nonfunctioning pituitary macroadenomas: effect on tumor volume and lack of correlation with immunohistochemistry and somatostatin receptor scintigraphy. *J Clin Endocrinol Metab* 1994;79:1416–23.
19. Fusco A, Giampietro A, Bianchi A, et al. Treatment with octreotide LAR in clinically non-functioning pituitary adenoma: results from a case-control study. *Pituitary* 2012;15:571–8.
20. Chen J, Hersmus N, Van Duppen V, et al. The adult pituitary contains a cell population displaying stem/progenitor cell and early embryonic characteristics. *Endocrinology* 2005;146:3985–98.
21. Dominici M, Le Blanc K, Mueller I, et al. Minimal criteria for defining multipotent mesenchymal stromal cells. The International Society for Cellular Therapy position statement. *Cytotherapy* 2006;8:315–7.
22. Del Gobbo A, Vaira V, Guerini Rocco E, et al. The oncofetal protein IMP3: a useful marker to predict poor clinical outcome in neuroendocrine tumors of the lung. *J Thorac Oncol* 2014;9: 1656–61.
23. Vitale G, Gaudenzi G, Dicitore A, et al.Zebrafish as an innovative model for neuroendocrine tumors. *Endocr Relat Cancer* 2014;21:R67–R83.
24. Nicoli S, Presta M. The zebrafish/tumor xenograft angiogenesis assay. *Nat Protoc* 2007;2:2918–23.
25. Tobia C, Gariano G, De Sena G, et al. Zebrafish embryo as a tool to study tumor/endothelial cell cross-talk. *Biochim Biophys Acta* 2013;1832: 1371–7.
26. Horvath E, Kovacs K. Folliculo-stellate cells of the human pituitary: a type of adult stem cell?. *Ultrastruct Pathol* 2002;26:219–28.
27. Davis SW, Keisler JL, Pérez-Millán MI, et al. All hormone-producing cell types of the pituitary intermediate and anterior lobes derive from Prop1 expressing progenitors. *Endocrinology* 2016;157:1385–96.
28. Florio T, Thellung S, Arena S, et al. Somatostatin and its analog lanreotide inhibit the proliferation of dispersed human non-functioning pituitary adenoma cells in vitro. *Eur J Endocrinol* 1999; 141:396–408.
29. Yunoue S, Arita K, Kawano H, et al. Identification of CD133+ cells in pituitary adenomas. *Neuroendocrinology* 2011;94:302–2.
30. Mathioudakis N, Sundaresh R, Larsen A, et al. Expression of the pituitary stem/progenitor marker GFRα2 in human pituitary adenomas and normal pituitary. *Pituitary* 2015;18:31–41.
31. Fauquier T, Rizzoti K, Dattan M, et al. SOX2-expressing progenitor cells generate all of the major cell types in the adult mouse pituitary gland. *Proc Natl Acad Sci USA* 2008;105:2907–12.
32. Orciani M, Davis S, Appolloni G, et al. Isolation and characterization of progenitor mesenchymal cells in human pituitary tumors. *Cancer Gene Ther* 2015;22:9–16.
33. Yao Y, Tang X, Li S, et al. Brain tumor stem cells: view from cell proliferation. *Surg Neurol* 2009;71:274–9.
34. Alvarez CV, Garcia-Lavandeira M, Garcia-Rendueles ME, et al. Defining stem cell types: understanding the therapeutic potential of ESCs, ASCs, and iPS cells. *J Mol Endocrinol* 2012;49: R89–111.
35. Vankelecom H. Pituitary stem/progenitor cells: embryonic players in the adult gland?. *Eur. J. Neurosci* 2010;32:2063–81.
36. Di Ieva A, Rotondo F, Syro LV, et al. Aggressive pituitary adenomas-diagnosis and emerging treatments. *Nat Rev Endocrinol* 2014;10:423–35.
37. Molitch ME. Pharmacologic resistance in prolactinoma patients. *Pituitary* 2005;8:43–52.